Optimization of Cavity Designs of Tapered AlInAs/InGaAs/InP Quantum Cascade Lasers Emitting at 4.5 μm

Kamil Pierściński, Aleksandr Kuźmicz, Dorota Pierścińska, Grzegorz Sobczak, Maciej Sakowicz, Piotr Gutowski, Kamil Janus, Krzysztof Chmielewski, and Maciej Bugajski

***Abstract*—In this work design, fabrication and characterization of mid-infrared AlInAs/InGaAs/InP QCLs taper quantum cascade lasers are presented. In order to increase output power while keeping good beam quality, taper design of resonator was used. We have studied devices emitting at 4.5 μm with different shapes (linear, concave and convex) and angles of taper waveguide section, to optimize the output beam parameters, namely M^2 and brightness. Experimental results demonstrate that convex geometry taper laser with 1.7° taper shows the best performance, the highest output power up to 5 W and the smallest horizontal beam divergence of 5.6° in the fundamental mode. This design is also characterized by the highest brightness.**

***Index Terms*—Cavity design, tapered laser, quantum cascade lasers.**

I. Introduction

QUANTUM cascade lasers (QCL) have a well-established position as mid-infrared sources with a large number of applications such as free space communication [1]–[3], absorption spectroscopy-based molecular sensing [4], breath analysis for medical diagnostics [5]. In most of the applications, lasing on the fundamental lateral transverse mode with narrow beam width and high output power is desirable. Such qualities are especially required by applications requiring precise collimation for beam delivery over long distances (e.g., free space optics – FSO systems).

Good quality of QCL beam can be obtained from device with narrow active region, but in such case, low output power is obtained. There are several methods to increase the output power of semiconductor laser. However, the straightforward solution of increasing the output power by increasing the ridge width results in drastic deterioration of beam quality, as the QC laser tends to operate on very high order transverse mode. On the other hand, one could use very long [6] (of the order of 1 cm), narrow cavity to increase power. This however complicates handling and mounting of the semiconductor chip possibly reducing the yield.

Several further modifications of QCL waveguide have been proposed in order to obtain high power mid-infrared sources with high beam quality. Solutions reported in the literature include QCLs based on angled cavity [7] or QCLs with taper cavity design [8]–[11]. Recently, another approach was reported, based on broad area quantum cascade lasers with high transverse mode selection: either broad area (BA) quantum cascade lasers with distributed sidewall loss [12] or BA with trenches generated by focused ion beam milling in small portions of the device [13].

In this work, we demonstrate experimental investigation of optimization of tapered laser cavity designs. Earlier reports concerning taper geometries, considered linear shape of taper section. We have designed, fabricated and analyzed devices with different taper shapes: linear, convex and concave.

Taper designs allow increasing the output power while maintaining fundamental TEM00 mode operation and are the trade-off between beam quality and emitted power. Additionally, tapered waveguides reduce optical intensity at the output facet, while keeping self-heating to a minimum for high-performance. Taper geometry laser consists of two sections: narrow ridge waveguide section allowing only TEM00 mode to propagate and tapered section in which the mode is adiabatically expanded, allowing to reach high optical output power.

II. Investigated Devices

The heterostructure of taper QCL used in this study was based on 4 quantum wells, double phonon resonance scheme. The active region contains 50 repetitions of period consisting of eleven pairs of $In_{0.36}Al_{0.64}As$ and $In_{0.67}Ga_{0.33}As$ layers, with opposite strain. The active region was sandwiched between two $In_{0.53}Ga_{0.47}As$: Si 500 nm core layers with $n = 4 \times 10^{16}$ cm^{-3}. The low doped, $n = 2 \times 10^{17}$ cm^{-3} InP substrate was used as lower waveguide layer, whereas the upper waveguide was formed by 2500 nm $In_{0.52}Al_{0.48}As$: Si layer doped to $n = 1 \times 10^{17}$ cm^{-3}. The structure was capped with 500 nm

Manuscript received February 5, 2019; revised April 26, 2019 and September 18, 2019; accepted September 26, 2019. Date of publication October 21, 2019; date of current version November 19, 2019. This work was supported by National Center for Research and Development (Poland) by project TECHMATSTRATEG: SENSE no. 1/347510/15/NCBR/2018 and under Grant LIDER/019/317/L-5/13/NCBR/2014. *(Corresponding author: Kamil Pierściński.)*

The authors are with the Institute of Electron Technology, Warsaw 02-668, Poland (e-mail: kamil.pierscinski@ite.waw.pl; aleksandr.kuzmicz@ite.waw.pl; dorota.pierscinska@ite.waw.pl; grzegorz.sobczak@ite.waw.pl; sakowicz@ite.waw.pl; gutowski@ite.waw.pl; kamil.janus@ite.waw.pl; kchmielewski@ite.waw.pl; bugajski@ite.waw.pl).

Color versions of one or more of the figures in this article are available online at http://ieeexplore.ieee.org.

Digital Object Identifier 10.1109/JSTQE.2019.2948500

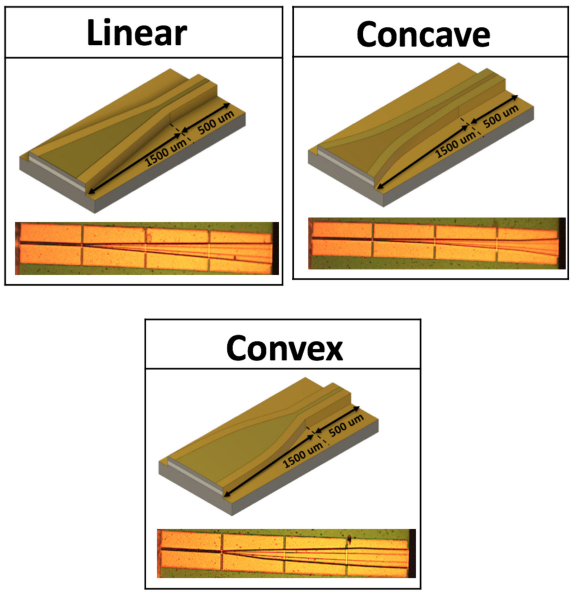

Fig. 1. Schematic picture and optical microscope image of a taper QCL with different geometries: linear, concave, convex.

InGaAs: Si, $n = 8 \times 10^{18}$ cm^{-3} top contact layer. The extensive description of the laser design can be found in papers [14]–[16]. Devices were designed for emission wavelength in the range of ~4.5 μm and grown by solid source Molecular Beam Epitaxy (MBE).

It is important to stress, that fabrication process of taper QCL is not different from standard ridge design by means of so called dry-etching process and does not require use of additional equipment (e.g., FIB -Focused Ion Beam) and time-consuming procedures. This allows high throughput and higher yield. The fabrication flow started with the definition of tapered quantum cascade laser geometries by conventional optical photolithography. Samples were then etched by deep RIE-ICP (Reactive Ion Etching - Inductively Coupled Plasma) etching in $CH_4/H_2/Cl_2/Ar$ gas mixture to obtain tapered ridge-type QCL waveguides. Deposition of Si_3N_4 main dielectric thin film was done by PECVD. Next, window was opened in dielectric by plasma etching. The top Ti/Pt/Au contact layers were deposited by magnetron sputtering and galvanic thickening of top gold layer. The processing was finalized after back contact (AuGe/Ni/Au) magnetron sputtering followed by RTA (Rapid Thermal Annealing) step. The last step is mounting of cleaved laser chips to AlN submounts and then to copper mounts.

Following the results of numerical simulations, tapered quantum cascade lasers were fabricated with three different geometries of waveguide: linear, concave and convex. The scheme of investigated geometries together with photographs from optical microscope are shown in Fig. 1.

Each of the shapes of taper were fabricated in variants of four taper angles varying between 0.4° and 3.6°. After fabrication, devices were investigated experimentally in terms of output power and beam quality. Top view of part of processed taper QCL wafer with linear taper geometry is shown in Fig. 2. It shows taper angles and corresponding widths of taper section at the front facet.

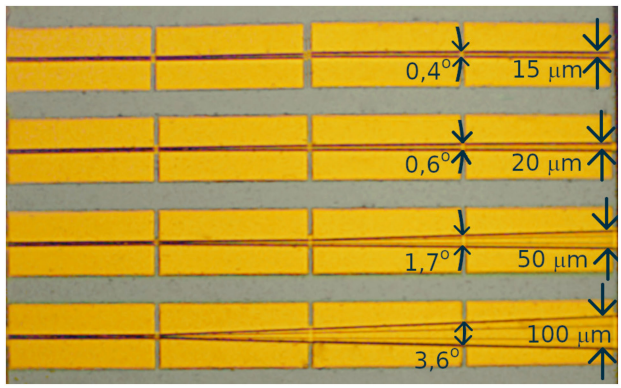

Fig. 2. Optical microscope image of part of processed taper QCL heterostructure with linear taper geometries with different taper angles 0.4°, 0.6°, 1.7° and 3.6°; 0.5 μm straight part and 1.5 μm taper part (ratio 1:3).

III. Numerical Results

Experimental works were preceded by systematic numerical simulations of optical mode propagation in different geometrical variants of the quantum cascade laser cavity. Numerical model was solved in COMSOL using Beam Propagation Method [17].

In numerical simulations the following parameters were assumed for the geometry of tapered QCLs; straight, narrow ridge section of 5 μm width and tapered section widths at the output mirror of 25, 50 and 100 μm, which correspond to taper angles of 0.6°, 1.7° and 3.6°, respectively.

To check how the section lengths ratio would influence the beam propagation and mode width at the output facet, for the case of concave taper, different ratios of section lengths were also investigated:

a) 500 μm length of narrow ridge section and 1500 μm length of taper section, denoted as 1:3;
b) 1000 μm length of both narrow ridge section and taper section, denoted as 1:1;
c) 1500 μm length of narrow ridge section and 500 μm length of taper section, denoted as 3:1.

Fig. 3 presents optical mode intensity distribution on the taper facet of QCL for concave geometries of the QCL cavity. Fig. 3(a) presents data for 25 μm width front facet with three ratios of section lengths, Fig. 3(b) for 50 μm width concave geometries also with three ratios of section length. Fig. 3(c) presents comparison of optical mode intensity distribution on the front facet (taper section) and rear facet (straight section) for concave geometry.

Numerical data shows that the ratio of section lengths (straight/taper) has little influence on optical mode width and distribution on the laser output facet. However, we clearly see that application of taper cavity design significantly increases horizontal mode size at the front facet. At the rear facet (straight section) the full width at half maximum (FWHM) of mode equals 3.5 μm, whereas at the front facet (taper section) the FWHM

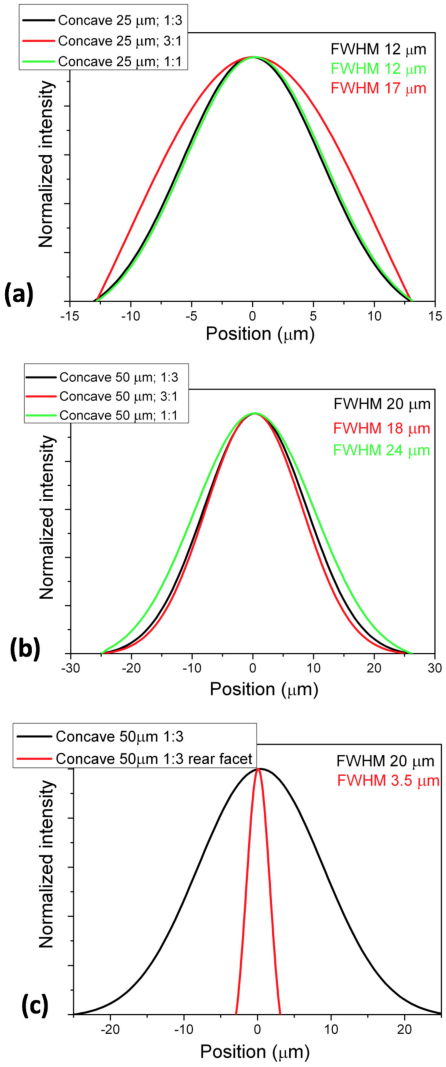

Fig. 3. Simulated optical mode intensity distribution on the taper facet of the cavity with different ratios of section lengths for (a) 25 μm width and (b) 50 μm width concave geometries.

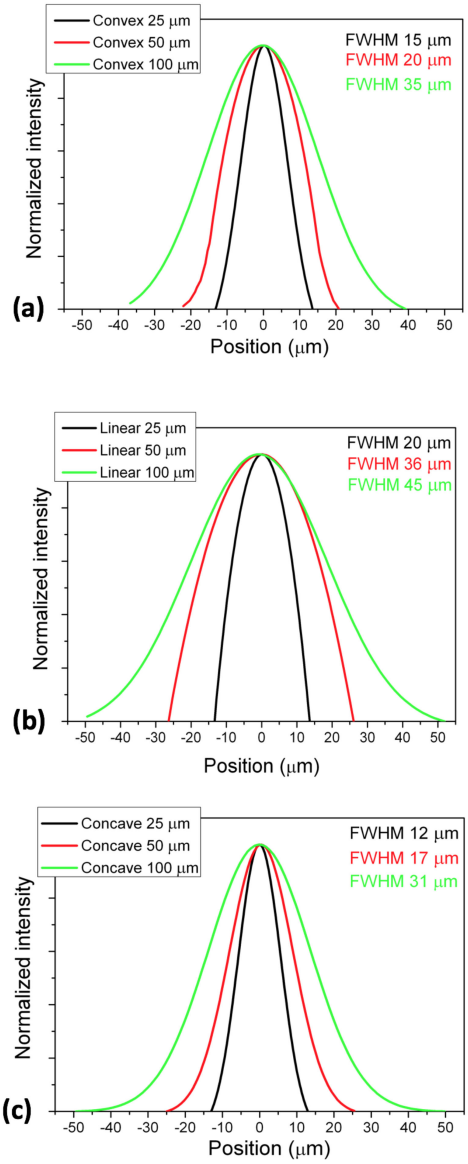

Fig. 4. Comparison of mode size at output facet for taper QCL of different geometries: (a) convex, (b) linear, (c) concave at different width(angle) of taper section.

of mode equals 20 μm. These results demonstrate that mode expansion occurs for all of investigated geometries.

In further numerical analysis and also in fabricated taper QCLs fixed length ratio 1 to 3 was used because such ratio has little influence on the mode size but significantly influences the value of emitted optical power [18].

Comparison of mode size for a fixed length ratio 1 to 3, at output facet for taper QCL with different geometries is shown in Fig. 4. The result for convex geometry is shown in Fig. 4(a), for linear in Fig. 4(b) and for concave in Fig. 4(c).

For all investigated geometries increase of the horizontal mode size with increase of angle of taper section was observed. (Fig. 5). In case of linear geometry, the highest width of the mode size on the output facet was observed: mode FWHM increases from 20 μm to 45 μm for width (angle) increasing from 25 μm (0.6°) to 100 μm (3.6°). Depending on geometry, 2.3–2.6 times extension of the mode size was observed.

Fig. 5 shows comparison of mode size on output facet for all investigated geometries for two widths of taper section: 25 μm width - Fig. 5(a) and for 100 μm width - Fig. 5(b). The increase of mode size on the output facet for linear shape of taper is 1.7 times larger than for convex shape in case of 25 μm width and 1.5 times larger in case of 100 μm.

The dependence between mode size and taper section width for all investigated configuration is summarized in Fig. 5(c). For all investigated shapes the increase of the mode size on the output facet in the function of taper section width (angle) is observed.

Numerical simulations show that the linear configuration of the taper QCL is characterized by the largest width of the mode, while the two configurations with the non-linear resonator shape (convex and concave) are characterized by smaller extension of the mode size.

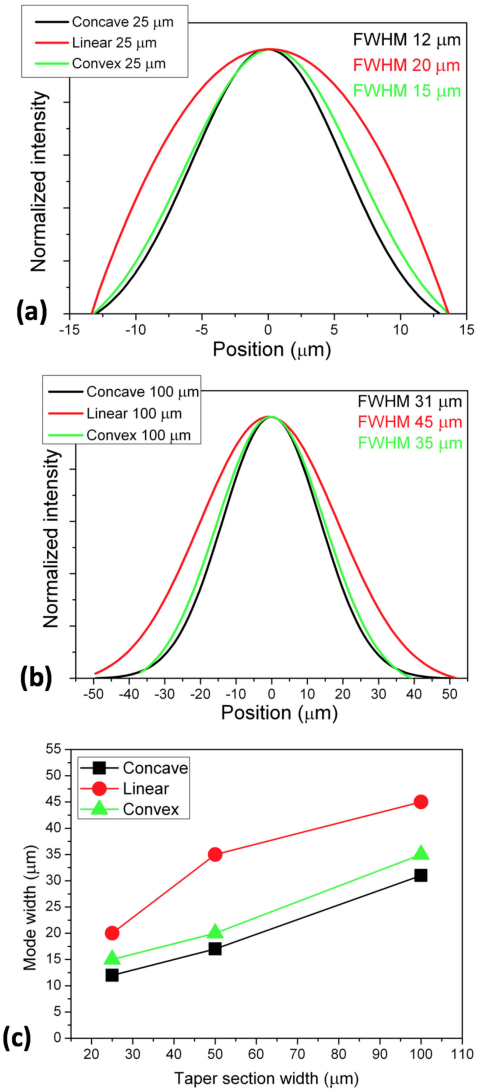

Fig. 5. Comparison of mode size on output facet for 25 μm width (a), and 100 μm width (b) taper section. (c) Dependence between mode size and taper section width for all investigated configuration.

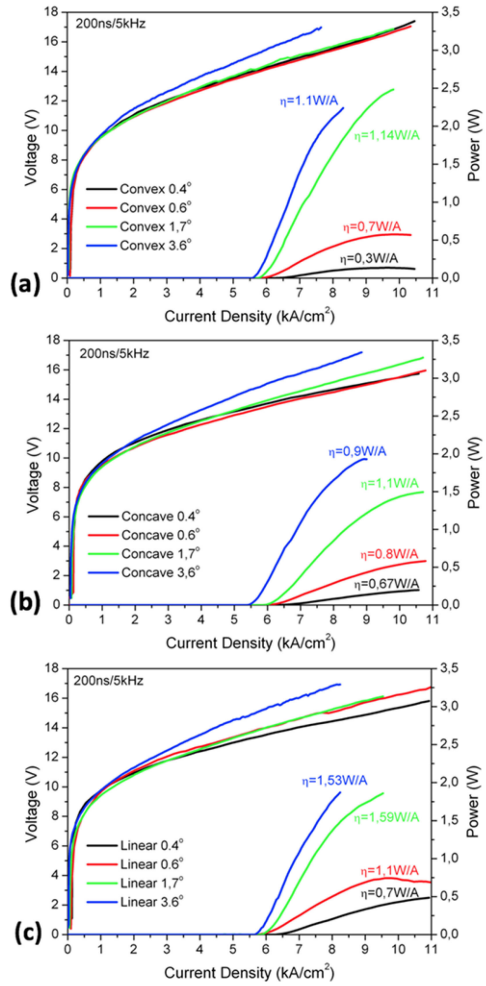

Fig. 6. LIV characteristics for convex (a), concave(b) and linear (c) designs of taper QCLs, with taper angle: 0.4°, 0.6°, 1.7°, 3.6°, register at room temperature with pulse width 200 ns and frequency 5 kHz.

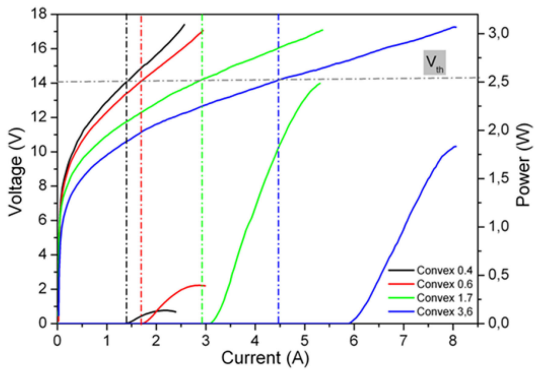

Fig. 7. Comparison of LIV characteristics for convex design of taper QCLs with taper angles of: 0.4°, 0.6°, 1.7°, 3.6°.

IV. Experimental Results

Based on the results of the numerical calculations, series of taper QCLs was fabricated.

Comparison of light-current-voltage (LIV) characteristics for convex, concave and linear designs of investigated QCLs with taper angle change in the range from 0.4° to 3.6° is shown in the Fig. 6. For all geometries, QCLs with 0.4° taper angle emitted the lowest output power and were characterized by the lowest value of slope efficiency. Also, for this angle we observed the highest threshold current density. With the increase of taper angle improvement of the parameters for all geometries was observed. However, experimental results show that there is an optimal value of the taper angle.

Fig. 7 presents LIV characteristics of convex-shaped taper QCLs. The value of V_{th} is marked in the graph, being the value of voltage reached at threshold current for the device with smallest taper angle. Since the threshold voltage in QCLs is connected with device design (geometry of the active region, type of the QW system design or number of stages in the active core), all geometries of taper are expected to have threshold currents at the same value of threshold voltage. However, it is clearly visible, that the threshold current increases with the increase of the taper angle, rapidly growing for the widest taper angle.

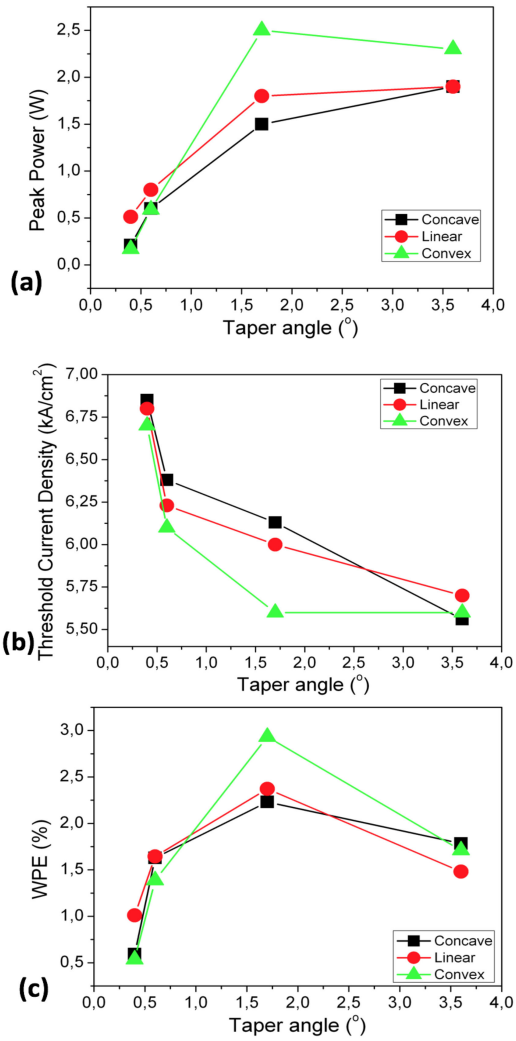

Fig. 8. Experimental dependence of emitted peak power (a), threshold current density (b), and WPE (c) extracted from experimental data of devices with various taper angles (widths) for all investigated taper geometries.

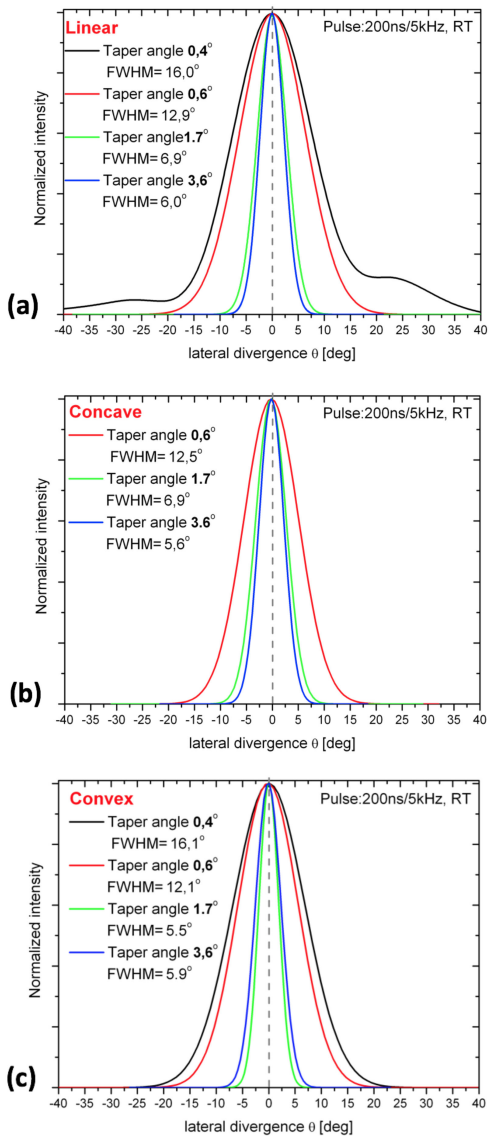

Fig. 9. Far-field profiles for three investigated geometries: linear (a), concave(b) and convex(c) at different taper angles change in the range from 0.4°–3.6°.

Increased threshold current indicates additional loss mechanism. In case of the widest devices, the optical mode is not filling the whole available active medium volume. This fact alone is responsible for observed decrease of the performance of the large angle devices of all designs. The excess electrical pumping is converted to excess heat and thus lowers the performance further.

Measured peak power, slope efficiency, threshold current density and wall-plug efficiency (WPE) as the functions of the taper width (angle) are presented in Fig. 8. WPE presented in Fig. 8 (c) should be doubled, as they were calculated considering power exiting from one mirror, since the devices were not HR coated. In case of narrow devices, the WPEs are lower, due to increased sidewall-scattering. This effect is mostly pronounced in case of narrow taper devices, as the relative influence of narrow straight section – just 5 micrometers wide – is the highest. In case of wider devices, the area of the taper is much greater, and the effect of sidewall scattering affects the performance less.

Increase of emitted power and slope efficiency for taper angle in range 0.4° – 1.7° is clearly visible. For 3.6° some deterioration of performance of devices is observed. Threshold current density decreases for taper angles in the range 0.4° – 1.7°. Again, for 3.6°, little or no change of threshold current density is observed. The best performance was reached for convex design with taper angle of 1.7° in terms of the highest emitted power (2.5 W) and the lowest threshold current density (5.55 kA/cm^2). From WPE graph (Fig. 8(c)), it follows that there is an optimal width of the facet of taper section. For all taper shapes, the best WPE is found around 1.7°. Above that value we observe a decrease of WPE. The observed decrease of the performance for the widest devices stems from the fact of increased waveguide loss, as well as thermal issues. We have used short pulses and low duty cycle in the experiments. However, in case of the widest devices, relatively high current is required to achieve lasing threshold (large area of the active region). Additionally, devices are epi-side up mounted, what impairs the dissipation of heat

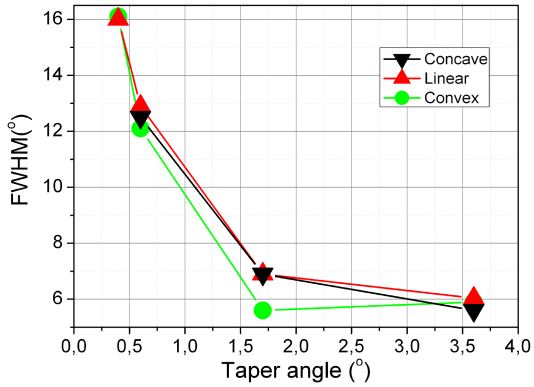

Fig. 10. FWHM angles versus the taper angle for investigated geometries of taper QCL.

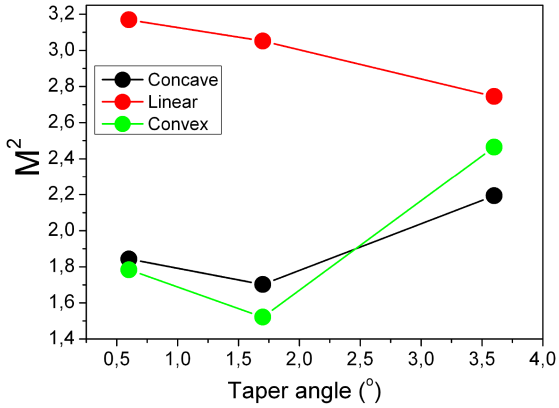

Fig. 12. Calculated M^2 parameter for three investigated geometries: linear, concave, convex at different taper angles change in the range from 0.6°–3.6°.

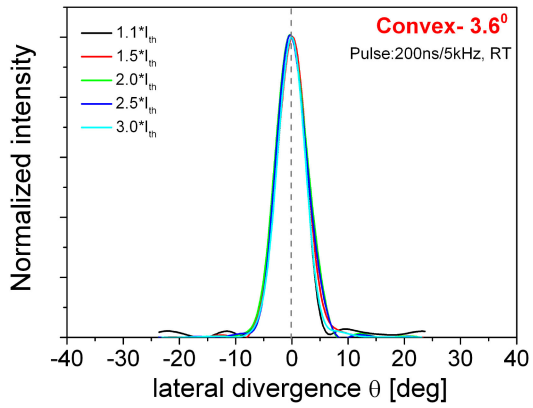

Fig. 11. Far field profiles registered for tapered (convex) QCL with 3.6° taper angle at increasing values of driving current showing stable emission pattern.

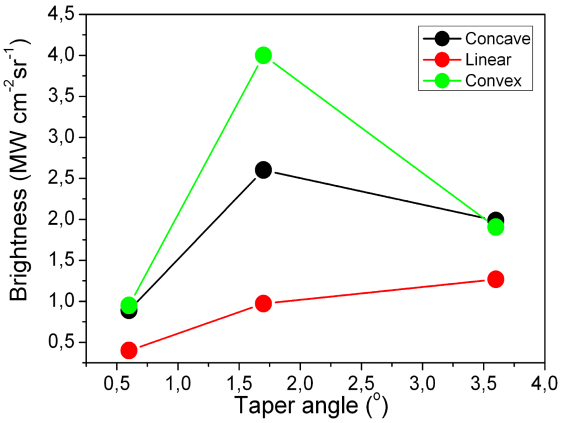

Fig. 13. Brightness values calculated for investigated geometries: linear, concave and convex for different taper angles in the range from 0.6°–3.6°. Modified, nonlinear tapers exhibit higher brightness values compared to linear design.

further. Both effects combined lead to effect of thermal roll-over, leading to observed decrease of the device performance.

To confirm and compare the performance of laser cavity designs of tapered quantum cascade lasers, it is necessary to measure far field intensity distribution. The measurements were performed by scanning the lateral field intensity by a detector placed on the rotation stage, such that the center of revolution is at the center of the laser output facet. Fig. 9 presents horizontal far-field profiles registered for different values of taper angle for three investigated geometries: linear, concave and convex. As expected, wider taper angle results in narrower horizontal far field profile for all investigated geometries of taper cavity design. The FWHM angles of registered optical field intensity profiles of the widest devices are 6° for linear shape, 5.6° for concave shape and 5.9° for convex shape. Dependence of FWHM angles on taper angle for investigated devices is shown in Fig. 10.

The use of taper geometry stabilizes the far field emission pattern of the device. Fig. 11 presents registered far field profiles as the function of driving current. One can observe, that far field profiles do not change their shape once the current is increased. This characteristic is crucial for optical systems, where beam stability is required.

Other important parameters used to describe laser beam quality and performance of semiconductor lasers are M^2 and brightness (B). M^2 parameter describes distortion of the beam in respect to the Gaussian beam, B parameter [19] describes useful power per area and solid angle and is given by:

$$B = \frac{P}{\lambda^2 M^2} \tag{1}$$

where P is the optical power, λ is the emission wavelength and M^2 is beam quality factor. M^2 is calculated according to:

$$M^2 = \frac{4\pi\sigma_{NF}\sigma_{FF}}{\lambda} \tag{2}$$

where σ_{NF} is the standard deviation of the calculated near field profiles of the fundamental lateral mode and σ_{FF} is the standard deviation of measured far field profile [20]–[22].

Calculated values of M^2 and brightness B parameter for investigated taper geometries: linear, concave and convex are presented in Fig. 12 (M^2) and Fig. 13 (B). M^2 and B values were calculated for different taper angles in the range from 0.6°–3.6°. Figures show the most important change resulting from the use of non-linear resonators of taper QCL. For convex

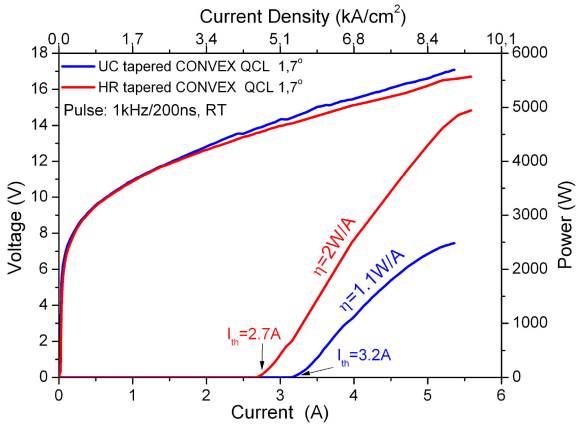

Fig. 14. Comparison of LIV characteristics for the best uncoated vs HR coated 1.7° taper angle convex QCLs.

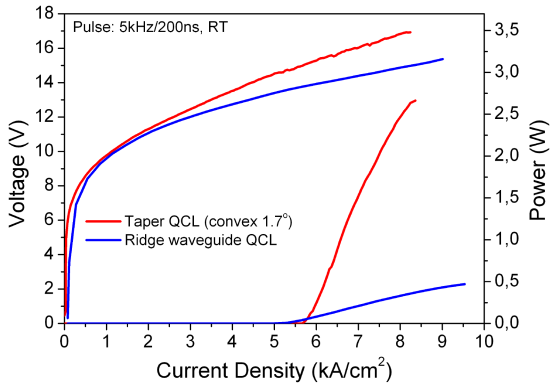

Fig. 15. Comparison of LIV characteristics for RW QCL 5 μm width and tapered (convex) QCL, with 3.6° taper angle, fabricated from the same InAlAs/InGaAs/InP heterostructure.

TABLE I
COMPARISON OF PARAMETERS OF THE UNCOATED VS. HR COATED 1.7° TAPER ANGLE CONVEX QCLS

Symbol	UNCOATED CONVEX 1.7°	HR COATED CONVEX 1.7°
Power	2.5 W	5 W
Slope Efficiency	1.1 W/A	2 W/A
WPE	3.1 %	5.9 %
M^2	1.7	1.7
Brightness	4.1 MW/cm^{2}sr	8.7 MW/cm^{2}sr

geometries with 1.7° the smallest value of M^2 parameters is obtained, equal to 1.5, and the highest value of brightness factor of 4.1 MW/cm^{2}sr. For concave geometry with 1.7° $M^2 = 1.7$ and $B = 2.6$ MW/cm^{2}sr were obtained. It is worth noting that for all taper angles, both non-linear shapes of the resonator, convex and concave, are characterized by much better value of M^2 parameter and B factor than linear shape. In addition, we observe that the optimal angle of the taper section of the QCL equals 1.7°, for larger angle (wider stripes) deterioration of the main parameters is observed.

Results indicate that modified, nonlinear designs of the taper section improve the major beam parameters: the brightness and M^2 in comparison to linear design, with convex shape of 1.7° angle being the optimal design in terms of M^2 and brightness parameters.

The optimal taper lasers (convex with taper angle 1.7°), were also fabricated with HR coating on the back facet (facet of narrow section). Fig. 14 shows comparison of LIV data for uncoated and HR coated taper QCLs. In case of HR coated device, the output power is doubled, and the threshold current is lower by 0.5 A. The slope efficiency for HR coated device reaches 2 W/A and is nearly doubled as compared to uncoated device.

Table I summarizes the comparison of parameters of the uncoated vs HR coated 1.7° taper angle convex QCLs. It is worth to note, that for HR coated device the brightness parameter equals 8.7 MW/cm^{2}sr.

Fig. 15 presents the comparison of LIV characteristics for typical ridge waveguide and tapered QC lasers. Both devices were fabricated from the same epitaxial wafer. Ridge device was 5 μm wide and 2 mm long. Taper device was 2 mm long cavity with 1.5 mm taper section. Taper design allowed to reach output power higher by a factor of ~4 as compared to straight ridge waveguide device. Devices show very similar threshold current density of ~5.5 kA/cm^2.

V. CONCLUSION

We have designed, fabricated and characterized mid-infrared AlInAs/InGaAs/InP QCLs emitting at 4.5 μm with tapered waveguides. A number of devices were tested with different geometries of the taper section: linear, convex and concave with different taper angles. It is demonstrated that, with the proper choice of device geometry, it is possible to combine low M2 and high power. Experimental results demonstrate increase of emitted power and slope efficiency for taper angle in range 0.4° – 1.7° in case of all taper shapes. The bigger the taper angle, the higher optical power and slope efficiency. For the largest investigated taper angle of 3.6°, experimental results show slight deterioration of the performance: decrease of power and slope efficiency.

Our research shows that convex design with taper angle of 1.7° exhibits the highest emitted power (2.5 W) and has the lowest threshold current density (5.55 kA/cm^2).

Nonlinear taper designs show better performance in terms of M^2 and B parameters. For convex geometries with 1.7° we obtained the smallest value of M^2 parameters equals 1.5 and the highest value of brightness factors of 4.1 MW/cm^{2}sr, with HR coatings: 8.7 MW/cm^{2}sr.

Taper device geometry stabilizes also the far-field profile of emission. The intensity distribution does not change with the increase of the driving current.

REFERENCES

[1] M. Razeghi *et al.*, "High-power mid- and far- wavelength infrared lasers for free space communication," *Proc. SPIE*, vol. 6593, 2007, Art. no. 65931V-6.

[2] J. Mikołajczyk, "An overview of free space optics with quantum cascade lasers," *Int. J. Electron. Telecommun.*, vol. 60, no. 3, pp. 259–263, 2014.

[3] J. Mikołajczyk *et al.*, "Analysis of free-space optics development," *Metrol. Meas. Syst.*, vol. 24, no. 4, pp. 653–674, 2017.
[4] B. G. Lee *et al.*, "Widely tunable single-mode quantum cascade laser source for mid-infrared spectroscopy," *Appl. Phys. Lett.*, vol. 91, pp. 231101–231103, 2007.
[5] A. Schwaighofer, M. Brandstetter, and B. Lendl, "Quantum cascade lasers (QCLs) in biomedical spectroscopy," *Chem. Soc. Rev.*, vol. 46, pp. 5903–5924, 2017.
[6] A. Bismuto, S. Blaser, R. Terazzi, T. Gresch, and A. Muller, "High performance, low dissipation quantum cascade lasers across the mid-IR range," *Opt. Express*, vol. 23, no. 5, pp. 5477–5484, 2015.
[7] Y. Bai, S. Slivken, Q. Y. Lu, N. Bandyopadhyay, and M. Razeghi, "Angled cavity broad area quantum cascade lasers," *Appl. Phys. Lett.*, vol. 101, 2012, Art. no. 081106.
[8] L. Nählea, J. Semmel, W. Kaiser, S. Höfling, and A. Forchel, "Tapered quantum cascade lasers," *Appl. Phys. Lett.*, vol. 91, pp. 181122–181124, 2007.
[9] G. Yu *et al.*, "Tapered quantum cascade lasers operating at 9.0 μm," *J. Semicond.*, vol. 31, 2010, Art. no. 034008.
[10] P. Rauter *et al.*, "Single-mode tapered quantum cascade lasers," *Appl. Phys. Lett.*, vol. 102, pp. 181102–181105, 2013.
[11] B. Gökden *et al.*, "High-brightness tapered quantum cascade lasers," *Appl. Phys. Lett.*, vol. 102, 2013, Art. no. 053503.
[12] R. Kaspi *et al.*, "Distributed loss method to suppress high order modes in broad area quantum cascade lasers," *Appl. Phys. Lett.*, vol. 111, pp. 201109–201114, 2017.
[13] R. Kaspi *et al.*, "Extracting fundamental transverse mode operation in broad area quantum cascade lasers," *Appl. Phys. Lett.*, vol. 109, pp. 211102–211104, 2016.
[14] M. Bugajski, "Mid-IR quantum cascade lasers: Device technology and non-equilibrium green's function modeling of electro-optical characteristics," *Phys. Status Solidi B*, vol. 251, no. 6, pp. 1144–1157, 2014.
[15] A. Kolek, G. Hałdaś, M. Bugajski, K. Pierściński, and P. Gutowski, "Impact of injector doping on threshold current of mid-infrared quantum cascade laser - non-equilibrium green's function analysis," *IEEE J. Sel. Topic Quantum Electron.*, vol. 21, no. 1, pp. 124–133, Jan./Fab. 2015.
[16] P. Gutowski *et al.*, "MBE growth of strain-compensated InGaAs/InAlAs/InP quantum cascade lasers," *J. Cryst. Growth.*, vol. 466, pp. 22–29, 2017.
[17] 2019. [Online]. Available: https://www.comsol.com
[18] Y. F. Li *et al.*, "The output power and beam divergence behaviors of tapered terahertz quantum cascade lasers," *Opt. Express*, vol. 21, pp. 15998–16006, 2013.
[19] W. T. Masselink, M. P. Semtsiv, A. Aleksandrova, and S. Kurlov, "Power scaling in quantum cascade lasers using broad-area stripes with reduced cascade number," *Opt. Eng.*, vol. 57, 2018, Art. no. 011015.
[20] D. Heydari, Y. Bai, N. Bandyopadhyay, S. Slivken, and M. Razeghi, "High brightness angled cavity quantum cascade lasers," *Appl. Phys. Lett.*, vol. 106, 2015, Art. no. 091105.
[21] G. Hatakoshi, "Analysis of beam quality factor for semiconductor lasers," *Opt. Rev.*, vol. 10, pp. 307–314, 2003.
[22] A. E. Siegman, "Defining, measuring and optimizing laser beam quality," *Proc. SPIE*, vol. 1868, pp. 2–12, 1993.

Kamil Pierściński received the M.Sc. and Eng. degrees in physics from the Warsaw University of Technology, Warsaw, Poland, in 2004 and the Ph.D. degree (Hons.) in semiconductor laser physics from the Institute of Electron Technology, Warsaw, in 2009, where he currently holds a position of the Head of Design and Characterization of Optoelectronic Devices Laboratory in the group of Prof. M. Bugajski. From 2012 to 2013, he joined the group of Prof. E. Kapon at EPFL, Switzerland, as a Postdoctoral Researcher in the field of optically and electrically pumped wafer-fused VECSELs. His main research interests include optical spectroscopy of semiconductor materials and devices. Current research topics include electrical, spectral, and thermal characterization of semiconductor lasers with emphasis on QCLs.

Aleksandr Kuźmicz was born in 1981. He received the M.Sc. degree in physical and analytical chemistry from the University of Pittsburgh, Pittsburgh, PA, USA, in 2007 and the Ph.D. degree in physical chemistry from the University of Warsaw, Warsaw, Poland, in 2014. His Ph.D. thesis concerns solar cells based on titanium dioxide. From 2003 to 2007, he was a Research Assistant with the University of Pittsburgh, Pittsburgh, PA, USA. He was an Associate Scientist with Nanomix, Inc. Emeryville, CA USA from 2007 to 2008, then from 2009 to 2015 He was a Researcher/Scientist with University of Warsaw, Warsaw, Poland. Since 2015, he has been Assistant Professor with the Institute of Electron Technology, Warsaw, Poland.

Dorota Pierścińska received the M.Sc. and Eng. degree in physics from the Warsaw University of Technology, Warsaw, Poland, in 2002 and the Ph.D. degree in semiconductor laser physics from the Institute of Electron Technology (ITE), Warsaw, Poland, in 2007. She is an Assistant Professor in Photonics Department with ITE, where she has worked since joining in 2002. Her research interests focus on thermal and reliability studies of semiconductor lasers, as well as optical spectroscopy of semiconductor materials and devices. Currently, her work focuses on optimization of the design and fabrication of mid-IR QCLs.

Grzegorz Sobczak was born in Warsaw, Poland, in 1985. He received the M.Sc.Eng. degree in physics from the Warsaw University of Technology, Warsaw, Poland, in 2009 and the Ph.D. degree in physics from the Institute of Electronic Materials Technology (ITME), Warsaw University of Technology, Warsaw, Poland, in 2016. His Ph.D. research concerns phase locked laser diode arrays and improving the quality of semiconductor laser beams. He was an Engineer with the Department of Optoelectronics, ITME, from 2008 to 2009, then was a Research Assistant from 2009 to 2016 in the same department of ITME. Since 2016, he has been a Postdoctoral with the Department of Photonics, Institute of Electron Technology, Warsaw, Poland.

Maciej Sakowicz received the M.Sc. degree in physics and the Ph.D. degree in solid state physics from the University of Warsaw, Warsaw, Poland, in 2004 and 2008, respectively. After graduation, he spend one year in the group of Prof. W. Knap in Montpellier, France working as a Posdoctoral Researcher on THz detection by field effect transistors. From 2009 to 2012, he joined the group of Prof. C. Silva with the Universite de Montreal, Montreal, Canada as a Postdoctoral Researcher working on ultrafast spectroscopy of organic solar cells. From 2012 till 2018 he worked with the Institute of Electron Technology, Warsaw, Poland on THz and mid-IR quantum cascade lasers. Since the beginning of 2019, he has been with the Institute of High-Pressure Physics, Polish Academy of Sciences working on THz detection and emission from field effect transistors. He is the author or coauthor more than 50 publications on solid state physics, photonics and electronics. His current research interests include quantum cascade lasers, plasmonic THz detectors and emitters.

Piotr Gutowski received the M.Sc. and Eng. degrees in physics from the Warsaw University of Technology, Warsaw, Poland, in 2010. He is currently working toward the Ph.D. degree with the Laboratory of Molecular Beam Epitaxy. He worked with the Institute of Electron Technology, Warsaw, Poland, in Photonics Department led by Prof. M. Bugajski. His main research activities involve growth of semiconductor structures with particular focus on Quantum Cascade Lasers, both AlGaAs/GaAs and InAlAs/InGaAs material systems. In 2013, he has received stipend for Ph.D. students conducting innovative research in technical sciences funded in the framework of Polish Human Capital Program. He is a coauthor of several publications related to growth and physics of semiconductor devices.

Kamil Janus was born in Sieradz, Poland, in 1991. He received the B.Eng. degree in mechatronics from the Wrocław University of Science and Technology, Wrocław, Poland, in 2016, where he also received the M.Sc.Eng. degree in the same field in 2017, he is currently working toward the Ph.D. degree in electronics with the Institute of Electron Technology, Warsaw, Poland, where he has been a Researcher in Photonics Department led by Prof. M. Bugajski since 2017.

Krzysztof Chmielewski was born in Warsaw in 1994. He is a student at the Faculty of Advanced Technologies and Chemistry, Military University of Technology, Warsaw, Poland. Since 2014, he has been working as a Chemist with the Department of Photonics, the Institute of Electron Technology. He is a specialist of lithography and high quality processing of advanced optoelectronics devices.

Maciej Bugajski received the M.Sc. degree in solid state physics from the Warsaw University, Warsaw, Poland, the Ph.D. degree in electrical engineering and the D.Sc. degree in electrical engineering from the Institute of Electron Technology, Warsaw, Poland, in 1972, 1980, and 1985, respectively. In 1972, he joined the Institute of Electron Technology, to work on optical spectroscopy of excitons in III–V compounds and later on heterostructure semiconductor lasers. In 1976–1977, he spent one year as a Fulbright scholar with the Physics Department, the University of Illinois, Urbana-Champaign. In 1986–1988, he was a Visiting Scientist with the Department of Materials Science, Massachusetts Institute of Technology, Cambridge, MA, USA, where he worked on semi-insulating GaAs. He is currently the Head of Photonics Department with the Institute of Electron Technology. In 1992, he received Professor title and initiated works on molecular beam epitaxy and quantum well lasers. His current research interest is focused on mid-infrared quantum cascade lasers. He has authored more than 300 papers in semiconductor physics, crystal growth, device physics, and performance, and given more than 50 invited talks at conferences. He coauthored three books on semiconductor lasers. He received the Foundation for Polish Science Team Award (2005), the Polish Agency for Enterprise Development Award for quantum cascade lasers (2012), and Minister of Science and Higher Education Price for distinguished achievements in applied research (2013).